Jpn. J. Appl. Phys. Vol. 39 (2000) pp. 1186–1189
Part 1, No. 3A, March 2000

Study of Electronic Structures in $LaCo_{1-x}Ti_xO_3$ ($x = 0$, 0.05 and 0.15) Using Discrete-Variational-Xα Cluster Method

Hiroshi NAKATSUGAWA and Eisuke IGUCHI

Materials Science, Department of Mechanical Engineering and Materials Science, Faculty of Engineering, Yokohama National University, Tokiwadai, Hodogaya-ku, Yokohama 240-8501, Japan

(Received October 12, 1999; accepted for publication December 10, 1999)

Electronic structures of $[CoO_6]^{9-}$ clusters have been studied by *ab initio* molecular-orbital (MO) calculations using the discrete-variational (DV)-Xα cluster method in order to investigate the correlation between the change in the type of the majority carrier and electronic structures in $LaCo_{1-x}Ti_xO_3$ ($x = 0$, 0.05 and 0.15). The most significant features are that the $e_{g\uparrow}$ bandwidth in the $x \neq 0$ specimen is wide in comparison with the $x = 0$ specimen and the Co–O bonding MO energy levels in the $x \neq 0$ specimens are in the energy range of -3 eV to -2 eV. These calculations indicate that both the 3*d* electrons in donor centers of σ^* bands and the O 2*p* ligand holes in σ^* bands are responsible for the electronic conduction in the $x = 0.05$ and $x = 0.15$ specimens but the competition between the densities of 3*d* electrons in σ^* bands and O 2*p* ligand holes dominates the type of the majority carrier.

KEYWORDS: donor center, ligand hole, majority carrier, small polaron, molecular orbital, cluster method, discrete-variational Xα method

1. Introduction

Cobalt transition-metal oxides have been extensively studied for applications to new thermoelectric materials.[1–3] Among them, $LaCoO_3$ with a rhombohedrally distorted perovskite structure has been well known to show a thermally induced semiconductor-metal transition around 500 K. The ground state of Co^{3+} ions is nonmagnetic at low temperatures, and this state is generally termed a low-spin (LS) state because the crystal-field splitting ($10Dq$) larger than the Hund's-rule coupling results in t_{2g}^6-electronic configuration with a non-magnetic moment ($S = 0$) on Co^{3+}. As temperature increases from a very low temperature, the magnetic susceptibility in $LaCoO_3$ slowly increases and soon reaches a maximum at about 90 K, above which it follows the Curie-Weiss law in the temperature ranges of $150\,\mathrm{K} < T < 400\,\mathrm{K}$ with $\mu_{\mathrm{eff}} = 3.1\mu_{\mathrm{B}}$ and $650\,\mathrm{K} < T < 1200\,\mathrm{K}$ with $\mu_{\mathrm{eff}} = 4.0\mu_{\mathrm{B}}$, where μ_{eff} is the effective magnetic moment per Co ion. However, the question still remains: which spin state of Co^{3+} ion is predominantly responsible for such a high-temperature spin state in $LaCoO_3$, an intermediate-spin (IS) state ($t_{2g}^5e_g^1$: $S = 1$) or a high-spin (HS) state ($t_{2g}^4e_g^2$: $S = 2$):[4–7] Korotin *et al.*[8] recently demonstrated that the IS state was energetically competitive with the LS state, but was much more stabilised than the HS state. Furthermore, they also showed that the e_g orbital ordering in the IS state was responsible for the semiconducting nature below 500 K.[8] The spin-state transition associated with an appreciable local lattice distortion observed by Yamaguchi *et al.*[9] also ensures the effective action of Jahn-Teller distortion due to the IS state.

Our previous study[10] shows that the dominant conduction in $LaCoO_3$ at $T > 170\,\mathrm{K}$ is due to a hopping process of small polarons of holes in the narrow π^* bands. Electron-doped $LaCo_{1-x}Ti_xO_3$ also exhibits a similar polaronic conduction above 190 K.[11] Theoretically, electron doping enhances *n*-type semiconductivity but this is not realized in this system because the type of the majority carrier changes from negative to positive with increasing x.[11] Furthermore, the charge neutrality would require Co^{2+} ions as the amount of diamagnetic Ti^{4+} ions increases.[12] The large ionic size of Co^{2+} ions results not only in the increase of lattice constants but also a decrease in the rhombohedral lattice distortion. Therefore, the ground state in $LaCo_{1-x}Ti_xO_3$ must be different from $LaCoO_3$ because the magnitude for $10Dq$ decreases with increasing x. In fact, the LS-IS transition at 90 K does not occur in $LaCo_{1-x}Ti_xO_3$ ($x \neq 0$). Moreover, the magnetic susceptibility, χ, follows the Curie-Wiess law at $T > 130\,\mathrm{K}$ in the $x = 0.05$ specimen and at $T > 205\,\mathrm{K}$ in $x = 0.15$. These results yield $\mu_{\mathrm{eff}} = 3.2\mu_{\mathrm{B}}$ for $x = 0.05$ and $\mu_{\mathrm{eff}} = 2.7\mu_{\mathrm{B}}$ for $x = 0.15$.[11] Both the specimens exhibit a plateau in the $\chi^{-1} - T$ relationship between 350 K and 550 K.[12] The high-temperature spin state in $LaCo_{1-x}Ti_xO_3$ thus appears very similar to that of $LaCoO_3$. It is noteworthy that the magnitude for μ_{eff} decreases with increasing x in spite of the decrease in $10Dq$.

The primary aim of the present study is to investigate the relationship between the change in the type of the majority carrier and the electronic structures in $LaCo_{1-x}Ti_xO_3$ crystals. From this point of view, we have studied the electronic states in $LaCo_{1-x}Ti_xO_3$ ($x = 0$, 0.05 and 0.15) theoretically using the following computational method. Electronic structures are usually obtained by an *ab initio* molecular-orbital (MO) calculation based on the local-density approximation (LDA) of the density-functional theory (DFT). When an *ab initio* MO calculation is applied to strongly correlated electron systems, it usually faces several problems because the theoretically estimated *d*-*d* Coulomb interaction energy U is too small. In order to improve the LDA, Sarma *et al.*[13] employed the local-spin-density approximation (LSDA) approach, although one needs to employ the LSDA + U method in order to reproduce the magnitude of the band gap of the large U systems. Thus, in the present report we calculate the electronic structures in $LaCo_{1-x}Ti_xO_3$ within the framework of the LSDA approach using a discrete-variational (DV)-Xα cluster method which accounts very well for the electronic structures promoting the metal-insulator transitions in VO_2 and Ti_2O_3.[14,15] In the present calculation we use the *SCAT* program package for Microsoft Disk Operation System (MS-DOS) personal computers.[16]

2. Computational Procedures

The DV-Xα method, based on the self-consistent-field

Hartree-Fock-Slater (HFS) one-electron model[17] and the self-consistent-charge procedure,[18] is one of the most useful techniques for an approximate solution to the HFS equation. This method is one of the cluster methods using a local one-electron effective potential to approximate both the electron-correlation effect and the spin-correlation effect. In the LSDA approach, the effective Slater Xα exchange-correlation potential is given by $-3\alpha[3/8\pi\rho_{\uparrow\downarrow}]^{1/3}$, where $\rho_{\uparrow\downarrow}$ is the local spin density, and the exchange-scaling parameter α is fixed at 0.7 throughout the calculation. Since Adachi *et al.*[16] report the details of the computational treatments of the DV-Xα method, the present calculation follows their treatment.

The calculation of the electronic structures using the *ab initio* MO method has been carried out under the assumption that electronic structures of $[CoO_6]^{9-}$ clusters could be representative of those of $LaCo_{1-x}Ti_xO_3$ ($x = 0$, 0.05 and 0.15). Figure 1 shows the structure of the $[CoO_6]^{9-}$ cluster employed in the present calculation. This cluster involves 84 up or down spins. Furthermore, 48 numerical atomic basis functions, i.e., Co; $1s \sim 4p$ and O; $1s \sim 2p$, are used to expand the MO of the $[CoO_6]^{9-}$ cluster. These basis functions are the Slater-type orbital basis sets obtained from the short Herman-Skillman programs.[19]

$LaCo_{1-x}Ti_xO_3$ crystals have a pseudocubic perovskite structure with the rhombohedral distortion along the $\langle 111\rangle$ direction. Table I tabulates the lattice parameters of $LaCo_{1-x}Ti_xO_3$ ($x = 0$, 0.05 and 0.15) used in the calculation, i.e., the hexagonal cell parameters (a_H and c_H) and the primitive perovskite cell parameters ($a_P = b_P = a_H/\sqrt{2}$ and $c_P = c_H/2\sqrt{3}$) at room temperature which are quoted from refs. 10, 11 and 20. The unit cell employed in the *ab initio* MO calculation is composed of $3 \times 3 \times 3$ primitive perovskites, i.e., $La_{27}Co_{27-y}Ti_yO_{81}$ ($y = 0$ for $x = 0$, $y = 1$ for $x = 0.05$ and $y = 4$ for $x = 0.15$). The calculation of the Madelung potential requires a structure composed of $6\times6\times6$ unit cells because the crystallographic translational symmetry must be taken into consideration. As illustrated in Fig. 1, the $[CoO_6]^{9-}$ cluster is situated at the center of the $6\times6\times6$ structure, and the other Co^{3+}, Co^{2+}, Ti^{4+}, O^{2-} and La^{3+} ions in the rest of the $6\times6\times6$ structure are replaced by point charges ($+4e$ for Ti^{4+}, $+3e$ for Co^{3+} or La^{3+}, $+2e$ for Co^{2+} and $-2e$ for O^{2-}).

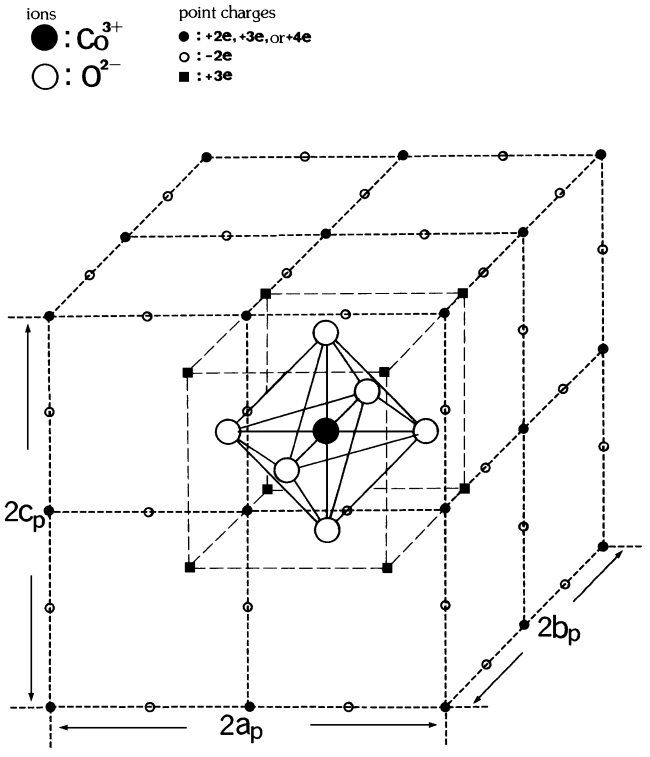

Fig. 1. Geometric structure of the cluster employed in the DV-Xα cluster method, i.e., $[CoO_6]^{9-}$ cluster which is employed in the calculations, where closed large circles indicate Co^{3+} ions and the open ones O^{2-} ions. This cluster is at the center of the structure determined by the primitive perovskite cell parameters a_P, b_P and c_P. Closed small circles indicate the point charges corresponding to Co^{3+}, Co^{2+} and Ti^{4+}, while open small circles and closed small squares indicate the point charges representing O^{2-} and La^{3+}, respectively.

Table I. Hexagonal and primitive perovskite cell parameters of $LaCo_{1-x}Ti_xO_3$.

	Hexagonal		Primitive	Perovskite
x	a_H (Å)	c_H (Å)	a_P, b_P (Å)	c_P (Å)
0	5.446	13.088	3.851	3.778
0.05	5.449	13.114	3.853	3.786
0.15	5.468	13.167	3.866	3.801

3. Results and Discussion

Using the DV-Xα cluster method, we have calculated the MO, energies and molecular coefficients mainly contributing to each MO for the ground states in the system. We assume that the discrete MO energy levels obtained here form continuous energy bands and that the zero energy level is at the highest occupied molecular orbital (HOMO). Furthermore, we have calculated the average net charges of atoms and the Co–O bond overlap population in the $[CoO_6]^{9-}$ cluster using Mulliken population analyses.[21] Table II tabulates the average net charges of Co and O atoms in the $[CoO_6]^{9-}$ cluster of $LaCo_{1-x}Ti_xO_3$ ($x = 0$, 0.05 and 0.15), and the magnitude of the average net charges which decrease with increasing x. This finding suggests the enhancement of Co $3d$–O $2p$ hybridization with increasing x. Hence, to trace the Ti-substitution effects, the electronic structure calculation of $LaCoO_3$ by the DV-Xα cluster method is also required along with the calculations of $LaCo_{0.95}Ti_{0.05}O_3$ and $LaCo_{0.85}Ti_{0.15}O_3$.

Figure 2 displays the discrete MO energy levels in $LaCoO_3$. In the energy range of -10 eV to 5 eV, the predominant atomic basis functions in each MO are Co; $3d$ and O; $2p$. This indicates that the electronic structure around the zero energy level consists of Co $3d$ and O $2p$ orbitals which are hybridized with each other. The energy difference between t_{2g} and e_g levels is approximately 2.5 eV, and the difference between Co $3d$ levels of up spins and down spins is about 3.5 eV. Thus, $10Dq$ in $LaCo_{1-x}Ti_xO_3$ is smaller than the Hund's-rule coupling energy at room temperature. Takahashi *et al.*[22,23] suggested that the spin-state transition at 90 K occurred mainly due to the Co–O bond length varying with temperature. This means that there is some correlation between the spin-state transition and the hybridization of Co $3d$ and O $2p$ orbitals. Figure 2 also shows the Co–O bond overlap population at each MO in the $[CoO_6]^{9-}$ cluster. The bond overlap populations are obtained by the overlap of the Gaussian func-

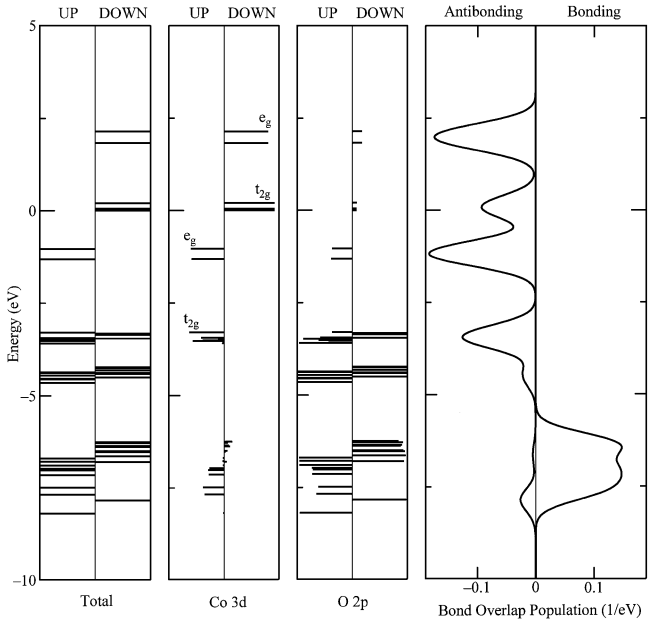

Fig. 2. Discrete MO energy levels (total, per Co 3*d* and O 2*p*, respectively) and Co–O bond overlap population at each molecular MO calculated for $LaCoO_3$ ($x = 0$).

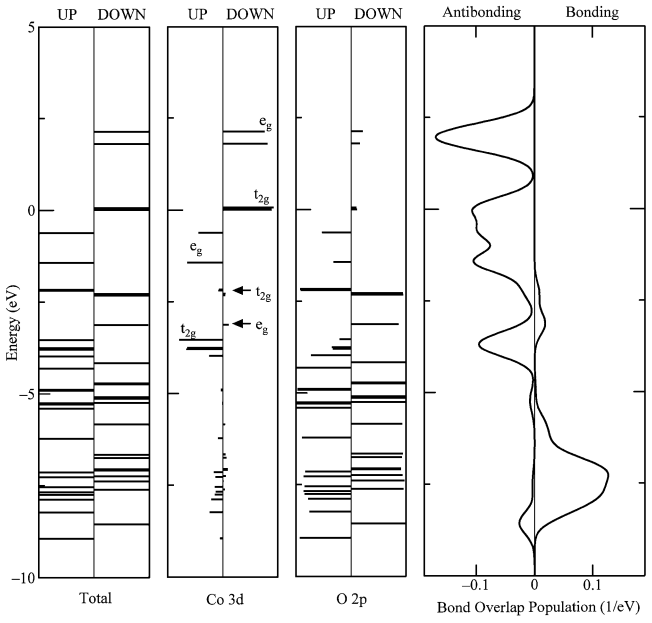

Fig. 3. Discrete MO energy levels (total, per Co 3*d* and O 2*p*, respectively) and Co–O bond overlap population at each molecular MO calculated for $LaCo_{0.95}Ti_{0.05}O_3$ ($x = 0.05$).

tions with a wide parameter of 0.5 eV, which are centered on each of the discrete MO energy levels. Thus, the energy levels near the zero energy level correspond to π^* or σ^* bands, where $*$ means the antibonding MO. In fact, the dominant conduction in $LaCoO_3$, above 170 K is due to the hopping process of small polarons of holes in the narrow π^* bands.[10)]

Figures 3 and 4 show the discrete MO energy levels (total, per Co 3*d* and O 2*p*, respectively) and the Co–O bond overlap population at each MO calculated for $LaCo_{1-x}Ti_xO_3$ ($x = 0.05$ and 0.15). The discrete MO energies at about 0 eV are mainly due to t_{2g} orbitals of down spins ($t_{2g\downarrow}$), both the energy levels at about -0.5 and -1.4 eV are mainly due to e_g orbitals of up spins ($e_{g\uparrow}$), and the energies in the range of -3 eV to -2 eV are mainly due to O 2*p* orbitals with $t_{2g\downarrow}$ and $e_{g\downarrow}$ symmetries. The most significant feature is that $e_{g\uparrow}$ bandwidth in $LaCo_{1-x}Ti_xO_3$ ($x = 0.05$ and 0.15) is wider than that of $LaCoO_3$ and the Co–O bonding MO energy levels in $x \neq 0$ are in the energy range of -3 eV to -2 eV. In addition, the intensity of the bonding overlap population for $x = 0.05$ is rather weak in comparison with the case of $x = 0.15$. In $LaCoO_3$, however, there is no bonding overlap population in this energy range. Therefore, these different electronic structures in $LaCo_{1-x}Ti_xO_3$ ($x = 0$, 0.05 and 0.15) indicate that the valence band structure changes as a function of x.

The dominant conduction in $LaCoO_3$ is due to the hopping process of small polarons of holes in the narrow π^* bands,[10)] while the type of the majority carrier changes from electrons to holes with increasing x from 0.05 to 0.15.[11)] According to Bahadur and Parkash,[12)] the negative Seebeck coefficient for $x = 0.05$ reflects the existence of donor centers, and the positive coefficient for $x = 0.15$ is caused by a decrease in the mobility of the electrons because carriers are trapped at Ti^{4+}–Co^{2+} clusters. Comparing the energy diagram of $LaCoO_3$ in Fig. 2 with the result for $x = 0.05$ in Fig. 3, we can locate the discrete MO energy level at -0.5 eV in the $x = 0.05$ specimen. Furthermore, this level is occupied by e_g electrons heavily hybridized with O 2*p* orbitals. The donor centers proposed by Bahadur and Parkash for $x = 0.05$ must correspond to this energy level. The thermal activation of 3*d* electrons in donor centers of σ^* bands is then likely to contribute to the electronic conduction in the $x = 0.05$ specimen.

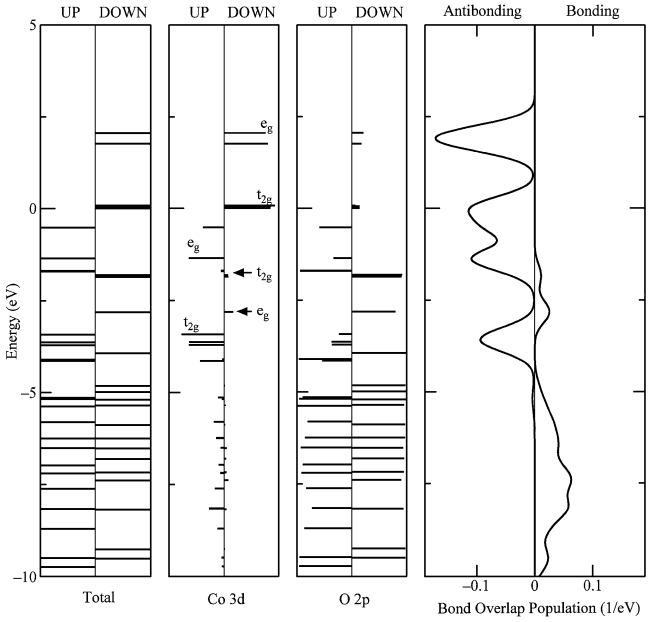

Fig. 4. Discrete MO energy levels (total, per Co 3*d* and O 2*p*, respectively) and Co–O bond overlap population at each molecular MO calculated for $LaCo_{0.85}Ti_{0.15}O_3$ ($x = 0.15$).

As x increases, the Co–O bond length at room temperature increases, as shown in Table I, but the magnitude for μ_{eff} decreases in spite of the decrease in $10Dq$.[11)] In $LaCoO_3$ ($x = 0$), the decrease in the Co 3*d*–O 2*p* hybridization could play an important role in the spin-state transition which is caused mainly by the Co–O bond lengthened by increasing temperature. Since the Co–O bond length increases in $LaCo_{1-x}Ti_xO_3$ with increasing x, as shown in Table I, one ex-

Table II. Average net charges of Co and O atoms in $[CoO_6]^{9-}$ cluster of $LaCo_{1-x}Ti_xO_3$.

x	Net charge of Co atom	Net charge of O atom
0	$+2.205e$	$-1.868e$
0.05	$+2.143e$	$-1.857e$
0.15	$+2.103e$	$-1.851e$

pects less hybridization of Co $3d$ and O $2p$ orbitals in $x \neq 0$ specimens. However, the present calculation indicates that Co $3d$–O $2p$ hybridization increases with increasing x. As illustrated in Figs. 3 and 4, the O $2p$ states with $t_{2g\downarrow}$ and $e_{g\downarrow}$ symmetries are responsible for the bonding MO in the energy range of -3 eV to -2 eV which is not included in $LaCoO_3$. Moreover, the bonding overlap population in this energy range increases with increasing x. These O $2p$ states must be the valence bands. As the experiments show, the type of majority carrier changes from negative to positive when x increases from 0.05 to 0.15.[11] This finding suggests that ligand holes are introduced in σ^* bands and the density of holes in the valence bands must exceed that of $3d$ electrons in σ^* bands when x increases from 0.05 to 0.15. The decrease in the average net charges shown in Table II is surely one of the predominant factors which enhances Co $3d$–O $2p$ hybridization. The heavy hybridization results in a ligand field strong enough to stabilize O $2p$ states with $t_{2g\downarrow}$ and $e_{g\downarrow}$ symmetries,[24] and then the O $2p$ ligand holes are responsible for the electrical transport in the $x = 0.15$ specimen. The stabilization of O $2p$ states with $t_{2g\downarrow}$ and $e_{g\downarrow}$ symmetries accounts very well for the decrease in μ_{eff} with increasing x in spite of the decrease in $10Dq$.

4. Conclusions

We have studied the electronic structure of the $[CoO_6]^{9-}$ cluster surrounded by a finite number of point charges in order to mimic the situation in $LaCo_{1-x}Ti_xO_3$ ($x = 0$, 0.05 and 0.15) crystals using the DV-Xα cluster method. The most significant features are that the $e_{g\uparrow}$ bandwidth in the $x \neq 0$ specimen is wider than that in $x = 0$ and the Co–O bonding MO energy levels in $x \neq 0$ are in the energy range of -3 eV to -2 eV. These results indicate that both the thermally activated $3d$ electrons in donor centers of σ^* bands and the O $2p$ ligand holes in σ^* bands are responsible for the electronic conduction in $x \neq 0$ specimens. Since the density of O $2p$ ligand holes is more than that of $3d$ electrons in σ^* when x increases from 0.05 to 0.15, the change in the type of majority carrier occurs.

Acknowledgments

This work was supported by a Grant-in-Aid for Science Research (No. 11650716) from the Ministry of Education, Science and Culture, and by Takahashi Industrial and Economic Research Foundation.

1) I. Terasaki, Y. Sasago and K. Uchinokura: Phys. Rev. B **56** (1997) R12685.
2) Y. Ando, N. Miyamoto, K. Segawa, T. Kawata and I. Terasaki: Phys. Rev. B **60** (1999) 10580.
3) T. Kawata, Y. Iguchi, T. Itoh, K. Takahata and I. Terasaki: Phys. Rev. B **60** (1999) 10584.
4) K. Asai, P. Gehring, H. Chou and G. Shirane: Phys. Rev. B **40** (1989) 10982.
5) M. Itoh, M. Sugahara, I. Natori and K. Motoya: J. Phys. Soc. Jpn. **64** (1995) 3967.
6) S. Yamaguchi, Y. Okimoto, H. Taniguchi and Y. Tokura: Phys. Rev. B **53** (1996) R2926.
7) T. Saitoh, T. Mizokawa, A. Fujimori, M. Abbate, Y. Takeda and M. Takano: Phys. Rev. B **55** (1997) 4257.
8) M. A. Korotin, S. Y. Ezhov, I. V. Solovyev, V. I. Anisimov, D. I. Khomskii and G. A. Sawatzky: Phys. Rev. B **54** (1996) 5309.
9) S. Yamaguchi, Y. Okimoto and Y. Tokura: Phys. Rev. B **55** (1997) R8666.
10) E. Iguchi, K. Ueda and W. H. Jung: Phys. Rev. B **54** (1996) 17431.
11) H. Nakatsugawa and E. Iguchi: J. Phys.: Condens.Matter **11** (1999) 1711.
12) D. Bahadur and Om. Parkash: J. Solid. State. Chem. **46** (1983) 197.
13) D. D. Sarma, N. Shanthi, S. R. Barman, N. Hamada, H. Sawada and K. Terakura: Phys. Rev. Lett. **75** (1995) 1126.
14) H. Nakatsugawa and E. Iguchi: Phys. Rev. B **55** (1997) 2157.
15) H. Nakatsugawa and E. Iguchi: Phys. Rev. B **56** (1997) 12931.
16) H. Adachi, M. Tsukada and C. Satoko: J. Phys. Soc. Jpn. **45** (1978) 875.
17) J. C. Slater: *Quantum Theory of Molecules and Solids* (McGraw-Hill, New York, 1974) Vol. 4 p. 1.
18) A. Rosën, D. E. Ellis, H. Adachi and F. W. Averill: J. Chem. Phys. **65** (1976) 3629.
19) F. Herman and S. Skillman: *Atomic Structure Calculations* (Prentice Hall, Englewood Cliffs, NJ, 1963) p. 1.
20) P. Ganguly, P. S. Anil. Kumar, P. N. Santhosh and I. S. Mulla: J. Phys.: Condens. Matter **6** (1994) 533.
21) R. S. Mulliken: J. Chem. Phys. **23** (1955) 1833.
22) H. Takahashi, F. Munakata and M. Yamanaka: Phys. Rev. B **53** (1996) 3731.
23) H. Takahashi, F. Munakata and M. Yamanaka: Phys. Rev. B **57** (1998) 15211.
24) F. Munakata, H. Takahashi and Y. Akimune: Phys. Rev. B **56** (1997) 979.